



A continuous fluidic bioreactor utilising electrodeposited silica for lipase immobilisation onto nanoporous gold

Xinxin Xiao, Till Siepenkötter, Robert Whelan, Urszula Salaj-Kośla, EDMOND MAGNER

Publication date

01-01-2017

Published in

Journal of Electroanalytical Chemistry; 812, pp. 180-185

Licence

This work is made available under the [CC BY-NC-SA 1.0](#) licence and should only be used in accordance with that licence. For more information on the specific terms, consult the repository record for this item.

Document Version

1

Citation for this work (HarvardUL)

Xiao, X., Siepenkötter, T., Whelan, R., Salaj-Kośla, U. and MAGNER, E. (2017) 'A continuous fluidic bioreactor utilising electrodeposited silica for lipase immobilisation onto nanoporous gold', available: <https://hdl.handle.net/10344/6297> [accessed 3 Mar 2023].

This work was downloaded from the University of Limerick research repository.

For more information on this work, the University of Limerick research repository or to report an issue, you can contact the repository administrators at ir@ul.ie. If you feel that this work breaches copyright, please provide details and we will remove access to the work immediately while we investigate your claim.

Post-printed version. Please refer this manuscript to: Xinxin Xiao, Till
Siepenkoetter, Robert Whelan, Urszula Salaj-Kosla, Edmond Magner; A
continuous fluidic bioreactor utilising electrodeposited silica for lipase
immobilisation onto nanoporous gold, *Journal of Electroanalytical Chemistry*
2017, doi: 10.1016/j.jelechem.2017.11.059

A continuous fluidic bioreactor utilising electrodeposited silica for lipase immobilisation onto nanoporous gold

Xinxin Xiao^a, Till Siepenkoetter^a, Robert Whelan^b, Urszula Salaj-Kosla^a and Edmond
Magner^{a,*}

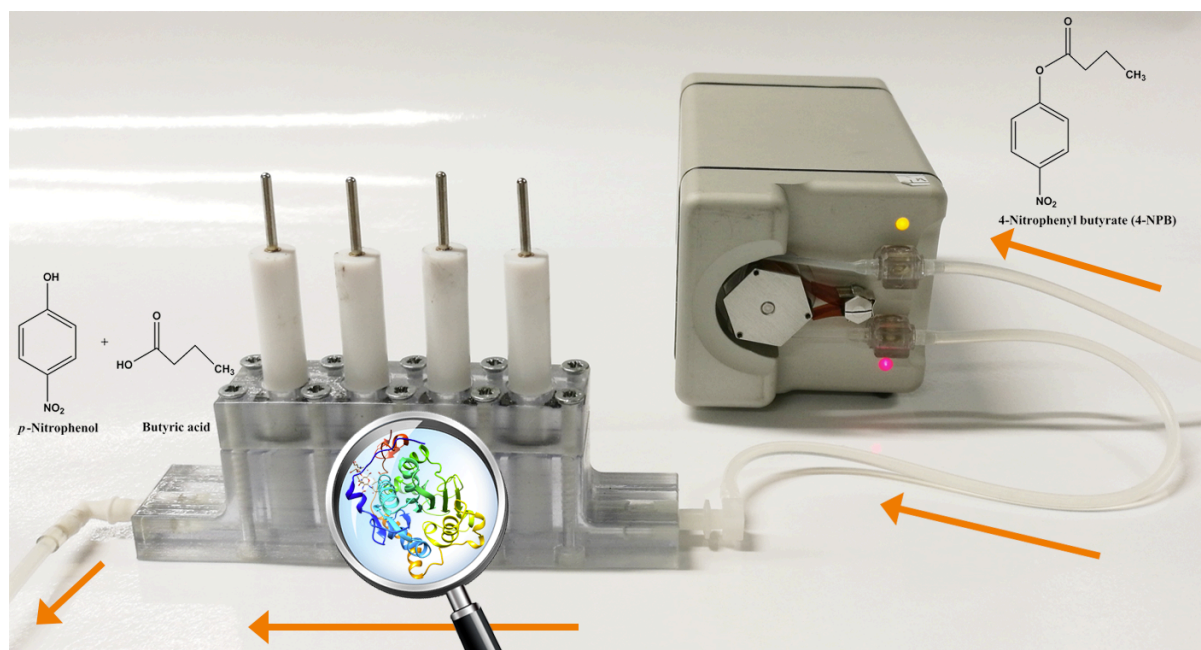
^aDepartment of Chemical Sciences and Bernal Institute, University of Limerick, Limerick,
Ireland

^bSchool of Design, University of Limerick, Limerick, Ireland

Keywords: lipase; electrodeposition; nanoporous gold; enzyme immobilisation; flow cell;
microfluidic enzymatic reactor

Abstract

An electrochemically triggered sol-gel process was used to generate a thin silica layer for the
immobilisation of lipase from *Thermomyces lanuginosus* onto dealloyed nanoporous gold
(NPG). The catalytic response of the entrapped lipase was examined using the hydrolysis of
4-nitrophenyl butyrate (4-NPB) as a model reaction. For the electrodeposition process,
parameters including the deposition time and the concentration of lipase affected the
observed catalytic activity. A deposition time of 180 s and a lipase concentration of 3 mg/mL
was used to prepare the optimised electrode. The operational stability of the silica
immobilised enzyme was enhanced on NPG in comparison to that on planar gold, which may
arise from confinement of the enzyme in the porous structure. The modified electrodes were
incorporated into a 3D printed flow cell with conversion efficiencies of up to 100% after 8
cycles.



1. Introduction

Immobilised enzymes [1] have been successfully used in applications such as biocatalysis [2, 3], biosensors [4] and biofuel cells [5-7]. Silicate materials including controlled pore glass (CPG), sol-gel derived silicate and mesoporous silicate (MPS) are biocompatible and widely used as solid supports for the immobilisation of enzymes [8]. Sol-gel derived silicate materials possess features that include ease of preparation, chemical inertness, negligible swelling and optical transparency [9]. In addition, the sol-gel process enables enzymes to be immobilised without significant losses in activity [10]. Electrodeposition provides a controllable and rapid route to grow uniform silica layers onto a conductive substrate regardless of the roughness of the surface [11]. The process of electrodeposition is initiated by an increase in pH in the proximity of the cathode as a consequence of hydrogen evolution, which consumes protons. Hydrolysis and condensation of precursors such as tetraethoxysilane (TEOS) are triggered by this change in pH [12], resulting in three-dimensional Si-O-Si networks that encapsulates enzyme in solution on the electrode/electrolyte interface.

A wide range of enzymes including glucose oxidases [13] and dehydrogenases [14, 15] *etc.* have been successfully immobilised in electrochemically generated silica matrices for use as biosensors. Various electrochemically derived sol-gel silica/nanomaterial hybrids, such as carbon nanotubes [16], gold nanoparticles [17], and macroporous gold electrodes [11], have been prepared. Nanoporous gold (NPG), fabricated by etching gold alloys, has been used as

a support material for the immobilisation of enzymes [18]. NPG possesses characteristic pores and ligaments whose sizes can be tailored by adjusting the dealloying conditions [19]. NPG has been modified with electrodeposited thin films of thiophene polymers [20] and Os modified polymers [5, 21] for the immobilisation of enzymes. In contrast to Os polymer modified electrodes that are prepared by drop-casting, electrodeposited films are more physically stable [22]. Electrodeposition enables control of the degree of modification of the entire surface [18] and the thickness of the deposited film can be tuned to optimise the enzyme loading [5].

Immobilisation makes it possible for enzymes to be used in a continuous flow mode [23]. In comparison to the conventional batch approach, flow methods are more efficient due to the large surface-to-volume ratio, ease of collection and on-line analysis of products [24]. Micro-reactors can be generally subdivided into three types: packed-bed, monolith and wall-coated reactors [25]. The former two can suffer from possible blockage and pressure gradients along the microchannels [26], making it difficult to tune flow dynamics. Inversely, wall-coated channels enable smoother flow with negligible mass transport resistance and thus predictable fluidic conditions. However, the catalyst loading of a wall-coated reactor is inferior to those of packed-bed and monolithic approaches [25], arising from the low working surface area. Porous supports can be used to improve the catalyst loading [27].

NPG electrodes with an average pore size of ca. 30 nm [5, 28] were functionalised by the electrodeposition of silica with simultaneous encapsulation of lipase [29] (Scheme 1). The bio-modified electrodes were placed into a bespoke flow channel device (Scheme 2). The hydrolysis of 4-nitrophenyl butyrate (4-NPB) by lipase was used as a model system (Scheme 3). The catalytic performance was affected by the thickness of the silicate layer and by the concentration of lipase. The conversion of substrate to product depended on the flow rate and full conversion was feasible upon recycling the solution.

2. Experimental section

2.1. Materials and apparatus

Potassium phosphate monobasic ($\geq 99\%$) and dibasic ($\geq 98\%$), hydrochloric acid (HCl, 37%), nitric acid (HNO₃, 70%), sulfuric acid (H₂SO₄, 97%), 4-nitrophenyl butyrate (4-NPB, $\geq 98\%$), Bradford reagent, bovine serum albumin (BSA, lyophilized powder, $\geq 96\%$) were obtained from Sigma-Aldrich Ireland, Ltd. Lipase (Sigma-Aldrich Ireland, Ltd) from

Thermomyces lanuginosus ($\geq 100 \text{ kUg}^{-1}$, EC no.: 3.1.1.3) was supplied as a solution containing 73% (w/v) water, 25% (w/v) propylene glycol, 2% (w/v) lipase, and 0.5% calcium chloride. 4-(2-Hydroxyethyl)-1-piperazineethanesulfonic acid (HEPES, $\geq 99\%$) and tetraethoxysilane (TEOS, 99.9%) were purchased from Fisher Scientific, Ireland. All solutions were prepared with deionised water (resistivity of $18.2 \text{ M}\Omega \text{ cm}$) from an Elgastat maxima-HPLC (Elga Purelab Ultra, UK).

NPG leaves were fabricated by etching ca. 100 nm thick Au/Ag leaf alloy films (12-carat, Eytzinger, Germany) in concentrated HNO_3 for 30 min at 30°C . The NPG films were then attached onto a pre-polished glassy carbon electrode (GCE) with a diameter of 4 mm and were allowed to dry. Before future utilisation, the NPG electrodes were activated by scanning the potential over the range of -0.2 to 1.65 V in 1 M H_2SO_4 at a scan rate of 100 mV s^{-1} for 15 cycles.

Electrochemical experiments were performed with a CHI802 potentiostat (CH Instruments, Austin, Texas) consisting of a NPG working electrode, a Pt wire counter electrode and a Ag/AgCl reference electrode. Samples mounted on 300-mesh copper grids (S147-3, Agar Scientific, UK) were characterised by transmission electron microscopy (TEM, JEOL JEM-2100, operating voltage of 200 kV). The average pore size and deposition layer thickness were measured with ImageJ software (National Institutes of Health, Bethesda, Maryland) [30]. Absorbance was recorded on a Cary 60 UV-Vis spectrophotometer (Agilent, USA).

2.2. Enzyme immobilisation procedures and activity measurement

A typical silica sol was prepared by dissolving 2.125 g tetraethoxysilane (TEOS), 2 mL of deionised water and 2.5 mL of 0.01 M aqueous HCl, which were mixed for 12 h using a magnetic stirrer and then diluted 3 times with water for further use. 900 μL of lipase solution in 0.1 M pH 7.0 phosphate buffer solution (PBS) was mixed with 100 μL of the above hydrolysed sol. A range of lipase concentrations was used. As shown in Scheme 1, sol-gel electro-assisted deposition was performed at an applied potential of -1.1 V vs. Ag/AgCl for different durations. The same route was applied to deposit silica/lipase onto planar gold electrodes (diameter: 3 mm) for comparison. Regeneration of the modified NPG electrodes was achieved by polishing and cleaning the glassy carbon electrode, followed by attachment of a new NPG film and subsequent deposition of silica.

All experiments were performed at room temperature (20 ± 2 °C). The activity of the immobilised lipase was evaluated by the hydrolysis of 4-NPB (Scheme 3). Flow experiments were performed by pumping buffer solution (10 mM pH 7.0 HEPES) containing 75 μ M 4-NPB at various flow rates (Scheme 2D). The system was washed (at a relatively fast flow rate of 0.12 mL min⁻¹ for 10 min) to allow the detachment of loosely-bounded enzymes prior to measurements. The absorbance of the product was measured at a wavelength of 420 nm. The stability of an electrode soaked in a solution of 4-NPB (2 mL, 75 μ M) at room temperature was checked once a day. Absorbance changes at 420 nm were recorded by immersing the electrode into a fresh solution (2 mL, 75 μ M 4-NPB) for one hour. To achieve 100% conversion of 4-NPB, the absorbance of the effluent solution was determined prior to recycling into the channel.

2.3. Flow cell design

Devices were designed using SolidWorks 3D CAD software (Dassault Systèmes, 2017). The flow cell consisted of two parts: a top-plate and a base (Scheme 2A). The top-plate was mounted above the base and fixed with 10 screws (Scheme 2D). Four NPG modified GCEs were inserted into the vertical holes of the device, sitting flush on top of a 500 μ m high channel (Scheme 2B). As shown in Scheme 2C, O-rings between the top-plate and base mitigated against any leakage of solution. A secondary function is that the action of tightening the top-plate onto the O-rings also caused the O-rings to squeeze the GCEs, effectively securing them in place on the top of the channel and preventing movement. An Instech P720 peristaltic pump was used to pump the solution into the channel (Scheme 2D) via round push-fit adaptors. The transition from a round adaptor to the laminar flow channel in the base was internally rounded to mitigate turbulence (Scheme 2C).

A Stratasys Objet Connex 500 3D printer featuring PolyJet Matrix™ Technology was used to print the flow cell parts with a laminar flow channel of a depth of 500 μ m. Printing was performed by successively laying down an acrylate based material (VeroClear RGD810) in 16 micron thick layers followed by UV curing and hardening of each layer. Exogenous material in cavities and overhangs was removed using a jet wash system. VeroClear RGD810 is a transparent material, that facilitates removal of the support material from the flow channel by allowing visual inspection of the jet washing step. This material also allows the visual detection of air bubbles forming inside the channel during operation.

2.4. Determination of immobilised protein concentration

The amount of immobilised lipase into the silica film onto the electrode was determined by the Bradford assay [31] of the initial and residual enzyme content in the electrodeposition solution. A range of concentrations of BSA from 0.15 to 1 mg mL⁻¹ in water were used to obtain the standard curve. The absorbances (595 nm) of mixtures of solutions of protein (50 uL) and Bradford reagent (1.5 mL) were measured.

3. Results and discussion

Application of a potential of -1.1 V vs. Ag/AgCl initiates the sol-gel process (Scheme 1) via the production of hydroxyl ions that trigger the condensation of TEOS. The deposition time was optimised using a solution containing 1 mg mL⁻¹ lipase. The effects of deposition time on the catalytic response are summarised in Fig. 1A. In agreement with previous studies [5, 20], the response increased with time for deposition times less than 180 s, and can be ascribed to the increased amount of enzyme immobilised. For longer deposition times, the response decreased which likely arise from limitations in the supply of 4-NPB supply to lipase. TEM images indicate that the thicker films block the pores (Fig. 2) [5]. A deposition time of 180 s was therefore utilised as a compromise between higher enzyme loading and mass-transport through the film. Similar phenomena were reported for the immobilization of *D*-sorbitol dehydrogenase [16] and of haemoglobin [11] in electro-deposited silica layers.

TEM confirmed the formation of a silica film on NPG (Fig. 2, Fig. S1). NPG (dark region of the micrographs) preserved its porous structure after electrodeposition with gold ligands growing thicker (Fig. S2). The relatively bright outer layer along the pores can be distinguished as the silica film with a uniform thickness. The optimal deposition time of 180 s resulted in a layer thickness of ca. 9.3±1.1 nm (in contrast to ca. 30 nm pores). A 60-s deposition time resulted in a 2.8±0.6 nm thick film (Fig. 2A), while the pores were filled after a deposition time of 360 s (Fig. 2C).

The effect of lipase concentration was optimised using a deposition time of 180 s. The catalytic response increased at lipase concentrations below 3 mg mL⁻¹ (Fig. 1B), at which point the response leveled off. Similar results were reported for the sol-gel deposition of *D*-sorbitol dehydrogenase on macroporous gold electrodes [14].

Silica/lipase was also deposited on a planar gold electrode using the optimised protocol (3 mg mL⁻¹ lipase, 180 s deposition time). Using the Bradford assay, the enzyme loading on planar

gold was determined to be 1.8 nmol cm^{-2} , in comparison to 3.6 nmol cm^{-2} on NPG. Despite a roughness factor of ca. 8 [28], NPG only encapsulated double the amount of lipase than that on the planar gold. This is likely due to the accelerated sol-gel process arising from the increased rate of hydrogen evolution that is observed on NPG in comparison to planar gold [32]. Similarly, Mazurenko et al. found that sol-gel derived bioelectrode performance was sensitive to the quantity of carbon nanotubes (CNTs) on the GCE as a high quantity of CNTs led to facilitated sol-gel process and faster silica film deposited [16]. When the stability of modified NPG and planar gold electrodes was examined (Fig. 3), NPG modified electrodes retained 49.3% of the original response after 5 h storage, in comparison to 20.2% on planar gold. The observed decrease in activity likely arises from loss of enzyme activity and/or leakage of the enzyme. Lipase can operate as a catalyst in aqueous and nonaqueous solutions in a stable manner [2]. For example, lipase that was physically adsorbed on NPG showed negligible activity loss after 10 successive uses, and maintained 74% of its initial activity after 20 cycles [33]. Lipase immobilised onto SBA-15 retained 95% activity after 7 cycles [2]. It is thus likely that the stability arises from leakage of the enzyme, especially given that sol-gel derived silica is generally brittle and can become cracked during long-term manipulation and use. The curved surface of NPG could provide a more stable environment for the film. Similar examples of enhanced stability on NPG have been observed. For example, electrodeposited MnO_2 on NPG preserved 64% of its capacitance after 50 cycles of charge-discharge, in comparison to 26% for planar Au/MnO_2 [21].

The dependence of the catalytic response of a single NPG/silica/lipase electrode on flow rates was examined over the range $0.01 - 0.12 \text{ mL min}^{-1}$ (Fig. 4). The catalytic response decreased with increasing flow rate due to the decreased residence time, in agreement with previous studies of lipase immobilized in flow reactors [34, 35].

Four NPG/silica/lipase electrodes were mounted in the flow cell (Scheme 2D). A linear increase in the amount of substrate conversion was observed in the first four cycles with the level of conversion leveling off in subsequent cycles. As can be seen from Fig. 5, the reaction was completed after eight cycles.

To examine enzyme leaching under flow conditions, a control experiment was performed by flushing the channel at a rate of 0.05 mL min^{-1} with blank PBS for 20 min. The solution collected (1 mL) was mixed with 1 mL of $75 \text{ }\mu\text{M}$ 4-NPB and incubated for 0.5 h. An absorbance change of 0.0054 (at 420 nm) was observed corresponding to leaching of 0.36%

of the enzyme. This result is consistent with the data in Fig. 3 that showed a decrease in activity with time. This leaching likely arises from removal of the silica from the electrode.

The NPG was physically attached on to the GCE and could be removed. Freshly prepared NPG leaves can be re-attached onto the GCE with newly generated silica layers to immobilise lipase. Fig. 6 shows the normalised activity of 10 regenerated NPG/silica/lipase electrodes. A RSD of 4.6% demonstrated the reproducibility of the method.

4. Conclusions

In this study, direct incorporation of lipase into sol-gel derived silica onto NPG was proposed. The effects of electrodeposition time and lipase concentration in the electrolyte on the catalytic response were systematically evaluated. The porous structure of NPG had a remarkable, positive influence in enhancing operational stability, although only a two-fold increase for the initial catalytic response over that on a planar Au electrode supported silica/lipase. The laminar flow cell allowed the study of the effect of flow rate. Operated in a loop mode at a flow rate of 0.05 mL min^{-1} enabled the complete hydrolysis of 4-NPB (2 mL of 75 μM solution) after eight cycles. The underlying study in the group is to integrate NPG supported enzymatic biofuel cells (EBFCs) with the bespoke flow cell.

Acknowledgments

This project has received funding from the European Union's Seventh Framework Programme for research, technological development and demonstration under grant agreement no 607793. X. Xiao acknowledges a Government of Ireland Postgraduate Scholarship (GOIPG/2014/659).

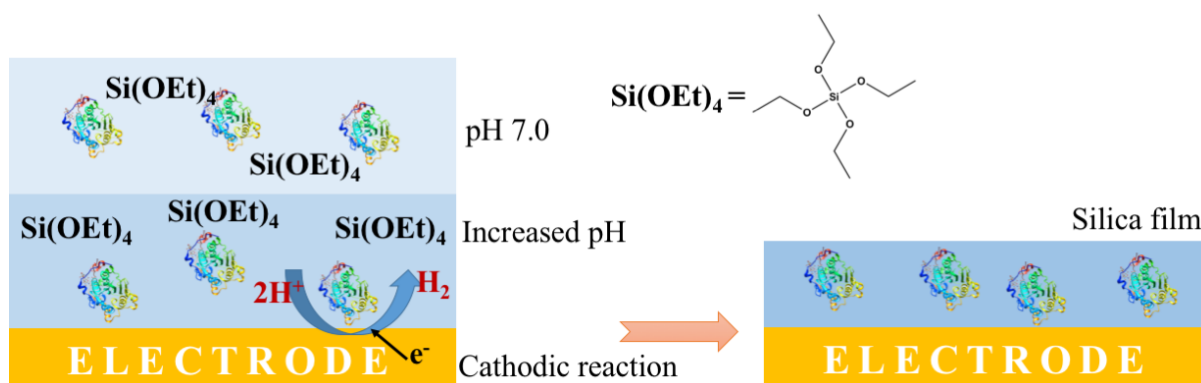
References

- [1] U. Hanefeld, L. Gardossi, E. Magner, Understanding enzyme immobilisation, *Chem. Soc. Rev.* 38(2) (2009) 453-468.
- [2] N.H. Abdallah, M. Schlumpberger, D.A. Gaffney, J.P. Hanrahan, J.M. Tobin, E. Magner, Comparison of mesoporous silicate supports for the immobilisation and activity of cytochrome c and lipase, *J. Mol. Catal. B: Enzym.* 108 (2014) 82-88.
- [3] R. DiCosimo, J. McAuliffe, A.J. Poulouse, G. Bohlmann, Industrial use of immobilized enzymes, *Chemical Society Reviews* 42(15) (2013) 6437-6474.
- [4] A. Heller, B. Feldman, Electrochemical Glucose Sensors and Their Applications in Diabetes Management, *Chem. Rev.* 108(7) (2008) 2482-2505.
- [5] X. Xiao, P.Ó. Conghaile, D. Leech, R. Ludwig, E. Magner, A symmetric supercapacitor/biofuel cell hybrid device based on enzyme-modified nanoporous gold: An autonomous pulse generator, *Biosens. Bioelectron.* 90 (2017) 96-102.

- [6] D. Leech, P. Kavanagh, W. Schuhmann, Enzymatic fuel cells: Recent progress, *Electrochim. Acta* 84(0) (2012) 223-234.
- [7] S. Calabrese Barton, J. Gallaway, P. Atanassov, Enzymatic Biofuel Cells for Implantable and Microscale Devices, *Chem. Rev.* 104(10) (2004) 4867-4886.
- 5 [8] E. Magner, Immobilisation of enzymes on mesoporous silicate materials, *Chem. Soc. Rev.* 42(15) (2013) 6213-6222.
- [9] W. Jin, J.D. Brennan, Properties and applications of proteins encapsulated within sol-gel derived materials, *Anal. Chim. Acta* 461(1) (2002) 1-36.
- [10] R. Gupta, N.K. Chaudhury, Entrapment of biomolecules in sol-gel matrix for applications in biosensors: Problems and future prospects, *Biosens. Bioelectron.* 22(11) (2007) 2387-2399.
- 10 [11] F. Qu, R. Nasraoui, M. Etienne, Y.B.S. Côme, A. Kuhn, J. Lenz, J. Gajdzik, R. Hempelmann, A. Walcarius, Electrogeneration of ultra-thin silica films for the functionalization of macroporous electrodes, *Electrochem. Commun.* 13(2) (2011) 138-142.
- [12] R. Shacham, D. Avnir, D. Mandler, Electrodeposition of Methylated Sol-Gel Films on Conducting Surfaces, *Adv. Mater.* 11(5) (1999) 384-388.
- 15 [13] W.-Z. Jia, K. Wang, Z.-J. Zhu, H.-T. Song, X.-H. Xia, One-Step Immobilization of Glucose Oxidase in a Silica Matrix on a Pt Electrode by an Electrochemically Induced Sol-Gel Process, *Langmuir* 23(23) (2007) 11896-11900.
- [14] Z. Wang, M. Etienne, G.-W. Kohring, Y. Bon-Saint-Côme, A. Kuhn, A. Walcarius, Electrochemically assisted deposition of sol-gel bio-composite with co-immobilized dehydrogenase and diaphorase, *Electrochim. Acta* 56(25) (2011) 9032-9040.
- 20 [15] Z. Wang, M. Etienne, F. Quilès, G.-W. Kohring, A. Walcarius, Durable cofactor immobilization in sol-gel bio-composite thin films for reagentless biosensors and bioreactors using dehydrogenases, *Biosens. Bioelectron.* 32(1) (2012) 111-117.
- [16] I. Mazurenko, M. Etienne, O. Tananaiko, V. Zaitsev, A. Walcarius, Electrophoretically deposited carbon nanotubes as a novel support for electrogenerated silica-dehydrogenase bioelectrodes, *Electrochim. Acta* 83 (2012) 359-366.
- 25 [17] R. Toledano, D. Mandler, Electrochemical Codeposition of Thin Gold Nanoparticles/Sol-Gel Nanocomposite Films, *Chem. Mater.* 22(13) (2010) 3943-3951.
- [18] X. Xiao, P. Si, E. Magner, An overview of dealloyed nanoporous gold in bioelectrochemistry, *Bioelectrochem.* 109 (2016) 117-126.
- 30 [19] T. Siepenkoetter, U. Salaj - Kosla, X. Xiao, S. Belochapkine, E. Magner, Nanoporous Gold Electrodes with Tuneable Pore Sizes for Bioelectrochemical Applications, *Electroanalysis* 28 (2016) 2415-2423.
- [20] X. Xiao, M.e. Wang, H. Li, P. Si, One-step fabrication of bio-functionalized nanoporous gold/poly (3, 4-ethylenedioxythiophene) hybrid electrodes for amperometric glucose sensing, *Talanta* 116(15) (2013) 1054-1059.
- 35 [21] X. Xiao, P.Ó. Conghaile, D. Leech, R. Ludwig, E. Magner, An oxygen-independent and membrane-less glucose biobattery/supercapacitor hybrid device, *Biosens. Bioelectron.* 98 (2017) 421-427.
- 40 [22] Z. Gao, G. Binyamin, H.H. Kim, S.C. Barton, Y. Zhang, A. Heller, Electrodeposition of Redox Polymers and Co - Electrodeposition of Enzymes by Coordinative Crosslinking, *Angew. Chem. Int. Ed.* 41(5) (2002) 810-813.
- [23] S. Kundu, A.S. Bhangale, W.E. Wallace, K.M. Flynn, C.M. Guttman, R.A. Gross, K.L. Beers, Continuous Flow Enzyme-Catalyzed Polymerization in a Microreactor, *J. Am. Chem. Soc.* 133(15) (2011) 6006-6011.
- 45 [24] Y. Asano, S. Togashi, H. Tsudome, S. Murakami, Microreactor technology: innovations in production processes, *Pharm. Eng.* 30(1) (2010) 32.
- [25] R. Munirathinam, J. Huskens, W. Verboom, Supported Catalysis in Continuous-Flow Microreactors, *Adv. Synth. Catal.* 357(6) (2015) 1093-1123.
- 50 [26] K. Szymańska, M. Pietrowska, J. Kocurek, K. Maresz, A. Koreniuk, J. Mrowiec-Białoń, P. Widłak, E. Magner, A. Jarzębski, Low back-pressure hierarchically structured multichannel microfluidic bioreactors for rapid protein digestion – Proof of concept, *Chem. Eng. J.* 287 (2016) 148-154.

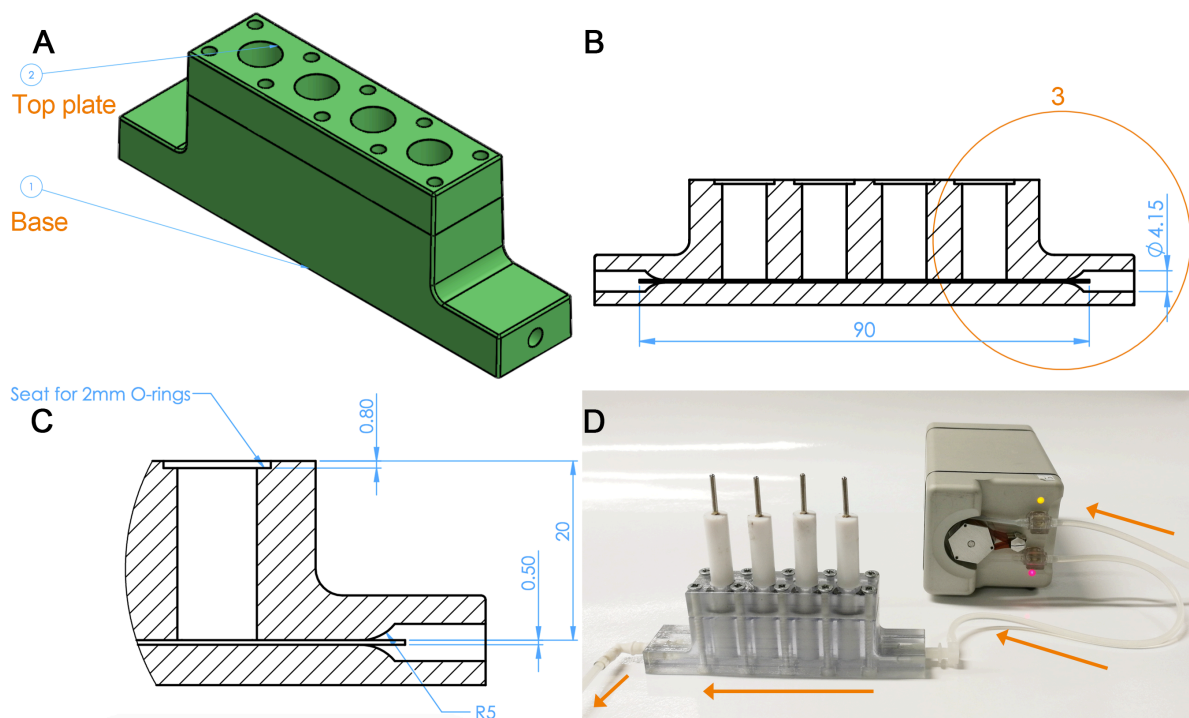
- [27] E.V. Rebrov, A. Berenguer-Murcia, H.E. Skelton, B.F.G. Johnson, A.E.H. Wheatley, J.C. Schouten, Capillary microreactors wall-coated with mesoporous titania thin film catalyst supports, *Lab on a chip* 9(4) (2009) 503-506.
- 5 [28] X. Xiao, J. Ulstrup, H. Li, J. Zhang, P. Si, Nanoporous gold assembly of glucose oxidase for electrochemical biosensing, *Electrochim. Acta* 130 (2014) 559-567.
- [29] I. Itabaiana, L.S. de Mariz e Miranda, R.O.M.A. de Souza, Towards a continuous flow environment for lipase-catalyzed reactions, *J. Mol. Catal. B: Enzym.* 85 (2013) 1-9.
- [30] C.A. Schneider, W.S. Rasband, K.W. Eliceiri, J. Schindelin, I. Arganda-Carreras, E. Frise, V. Kaynig, M. Longair, T. Pietzsch, S. Preibisch, NIH image to imageJ: 25 years of image analysis, *Nat. Methods* 9(7) (2012) 671.
- 10 [31] M.M. Bradford, A rapid and sensitive method for the quantitation of microgram quantities of protein utilizing the principle of protein-dye binding, *Anal. Biochem.* 72(1) (1976) 248-254.
- [32] X. Xiao, C. Engelbrekt, Z. Li, P. Si, Hydrogen evolution at nanoporous gold/tungsten sulfide composite film and its optimization, *Electrochim. Acta* 173 (2015) 393-398.
- 15 [33] X. Wang, X. Y. Liu, X. L. Yan, P. Zhao, Y. Ding, P. Xu, Enzyme-Nanoporous Gold Biocomposite: Excellent Biocatalyst with Improved Biocatalytic Performance and Stability, *PLoS ONE* 6(9) (2011) e24207.
- [34] I. Itabaiana, F.K. Sutili, S.G.F. Leite, K.M. Goncalves, Y. Cordeiro, I.C.R. Leal, L.S.M. Miranda, M. Ojeda, R. Luque, R.O.M.A. de Souza, Continuous flow valorization of fatty acid waste using silica-immobilized lipases, *Green Chem.* 15(2) (2013) 518-524.
- 20 [35] I. Denčić, S. de Vaan, T. Noël, J. Meuldijk, M. de Croon, V. Hessel, Lipase-Based Biocatalytic Flow Process in a Packed-Bed Microreactor, *Ind. Eng. Chem. Res.* 52(32) (2013) 10951-10960.

Figure Caption



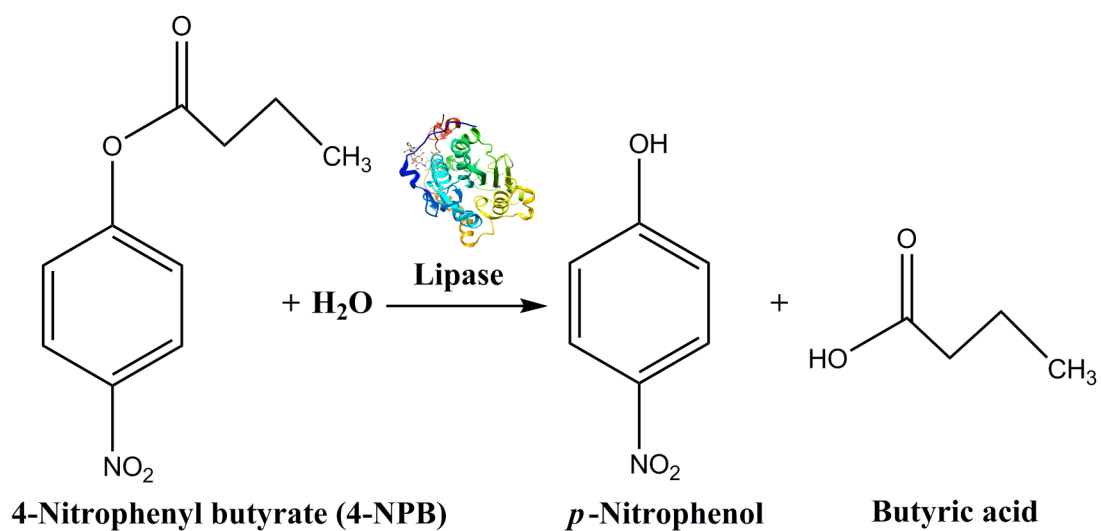
Scheme 1. Schematic drawing of the electrodeposition of silica for enzyme immobilisation at a constant negative potential.

5



Scheme 2. (A) CAD drawing of the flow cell consisting of top-plate and base. (B) Sectional view of the base (unit: mm). (C) Detailed view of part 3 from (B). (D) Photograph of the flow cell during operation; the arrows indicate the direction of flow.

10



Scheme 3. Hydrolysis reaction of 4-NPB catalysed by lipase.

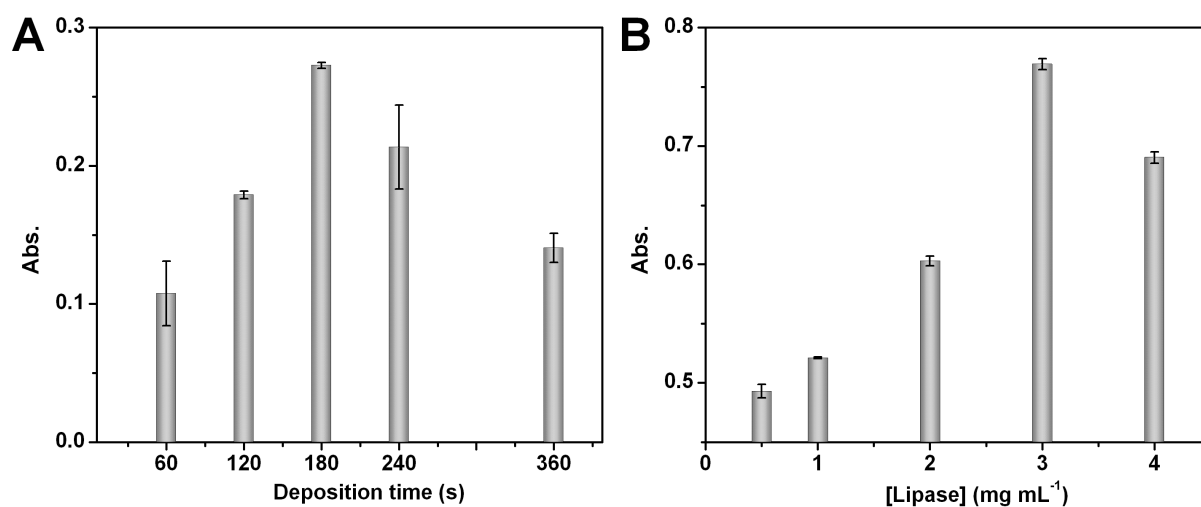


Fig. 1. (A) The effect of deposition time on the catalytic performance of NPG/silica/lipase obtained in 1 mg mL⁻¹ lipase (measured by immersion in 2 mL of 75 μM 4-NPB for 0.5 h). (B) The effect of lipase concentration on the catalytic performance of NPG/silica/lipase obtained by depositing for 180 s (measured by immersion in 2 mL of 75 μM 4-NPB for 1 h).

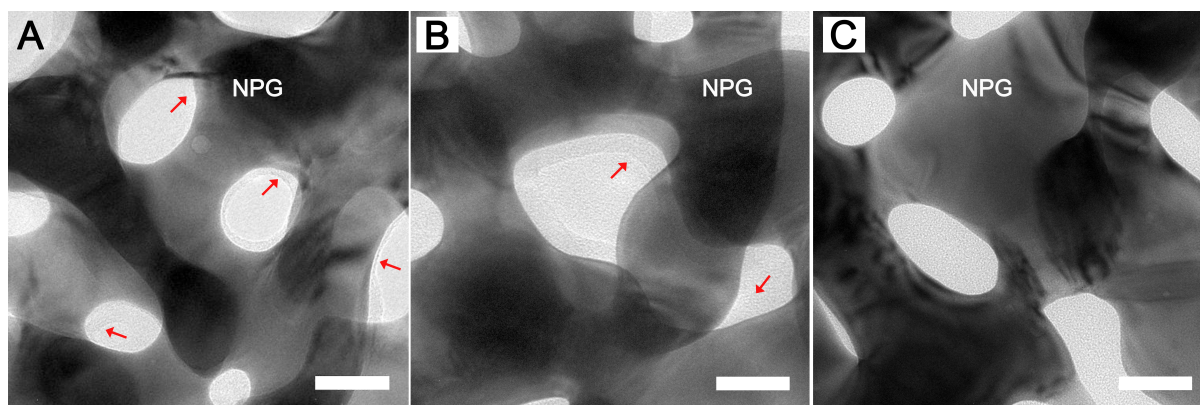


Fig. 2. TEM images showing the NPG/silica/lipase obtained in 1 mg mL⁻¹ lipase with various deposition durations: (A): 60 s, (B): 180 s, (C): 360 s; Arrow in (A) and (B) indicate the silica/lipase coating layers, while pores are filled with silica/lipase in (C); Scale bars at the right-bottom of (A), (B) and (C) indicate 30 nm.

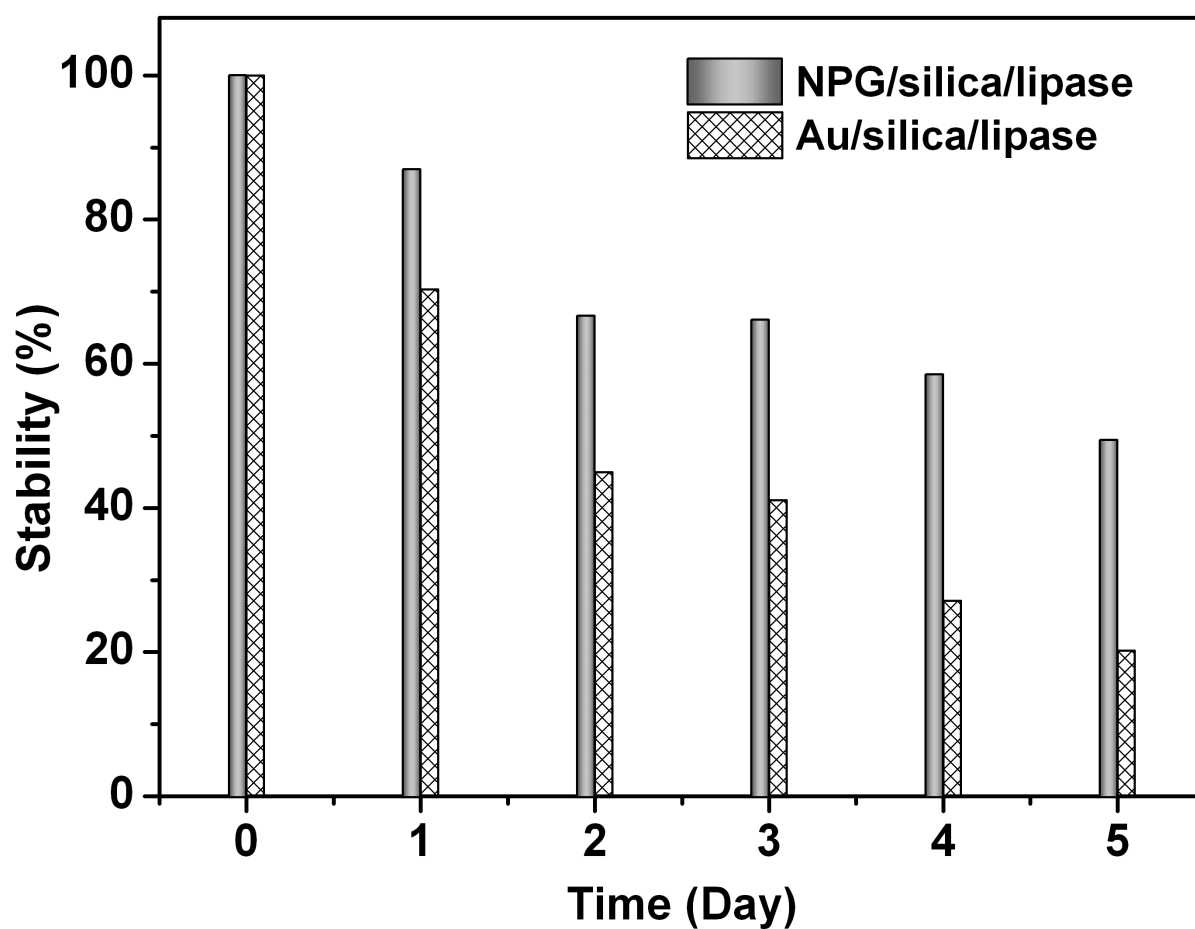


Fig. 3. Storage stability of NPG/silica/lipase; Response was measured by immersion in 2 mL of 75 μ M 4-NPB for 1 h.

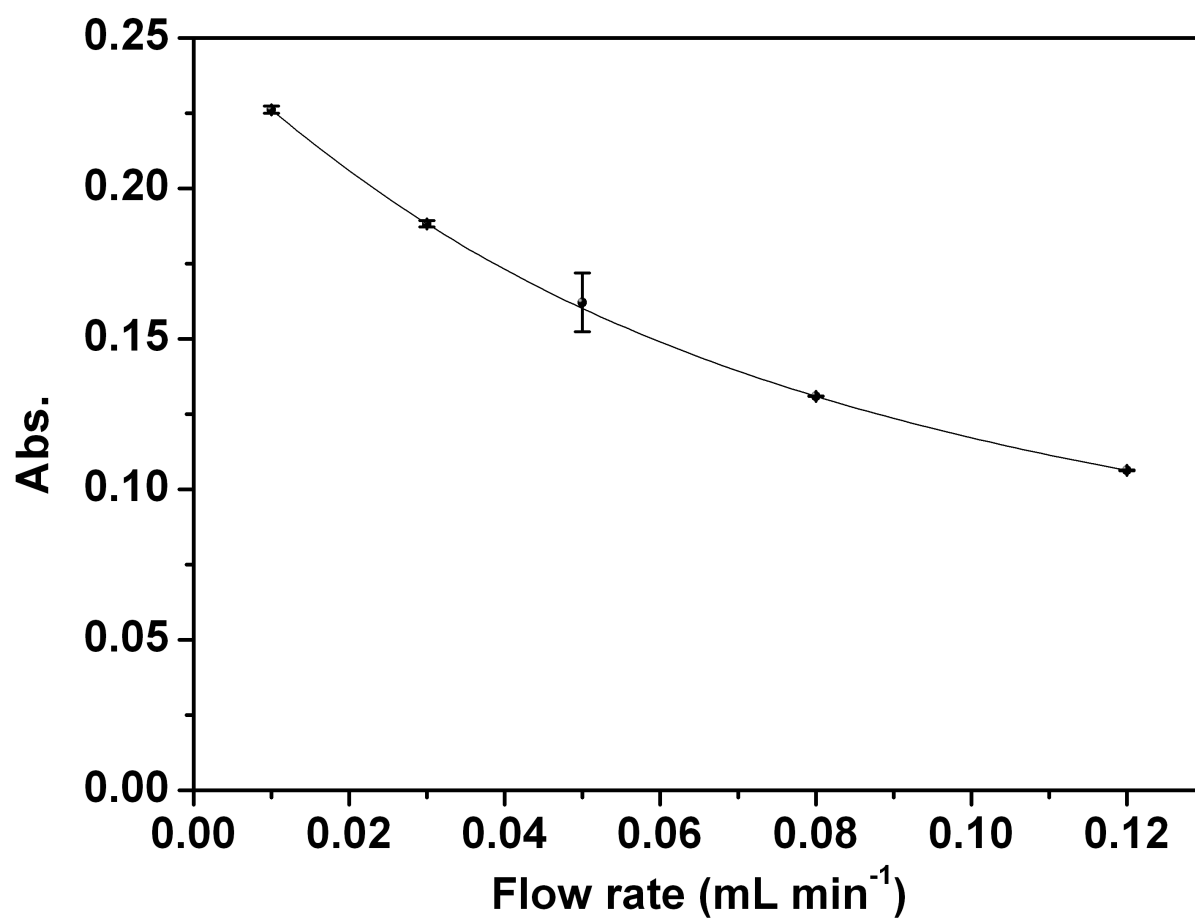


Fig. 4. The effect of flow rate at the catalytic behavior of NPG/silica/lipase towards 75 μ M 4-NPB.

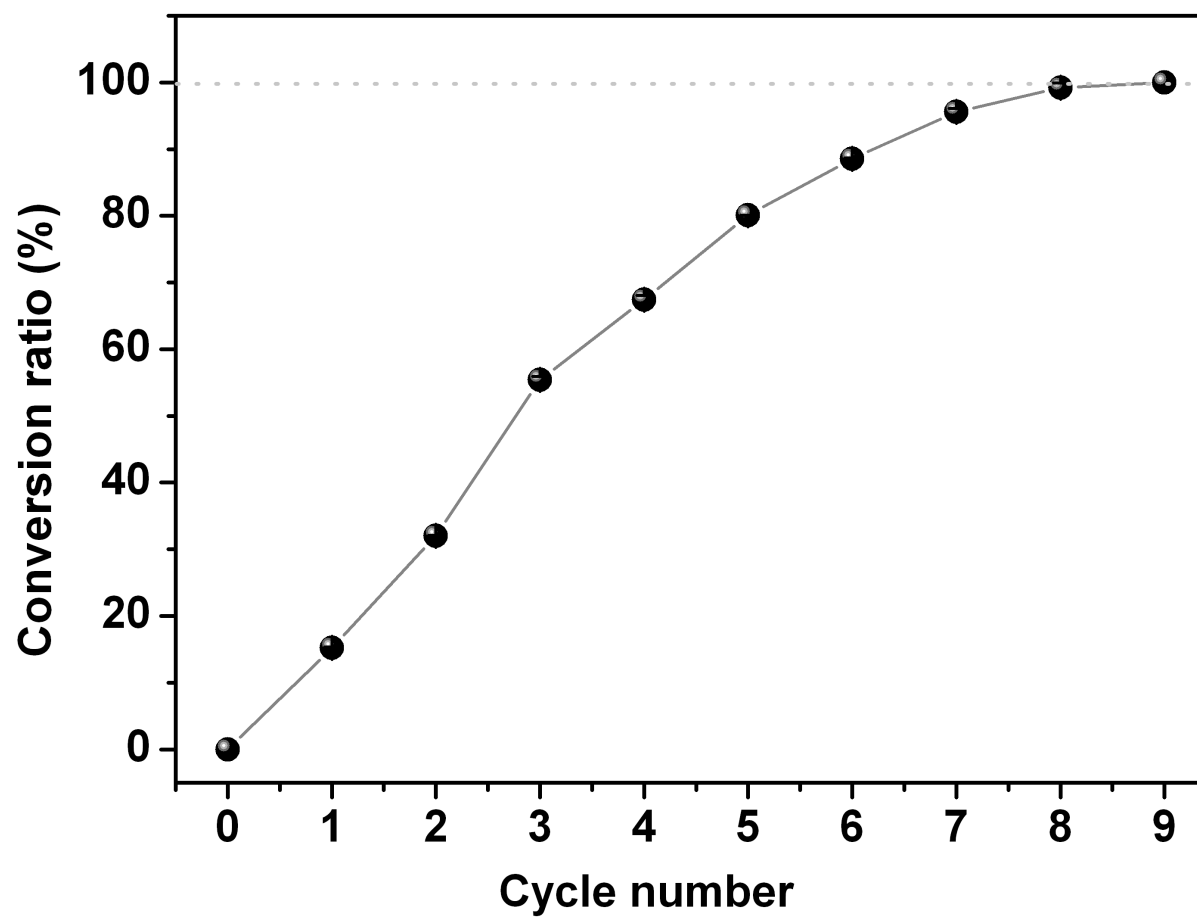


Fig. 5. Conversion ratio of 2 mL of 75 μ M 4-NPB by cycling in a loop at a flow rate of 0.05 mL min⁻¹.

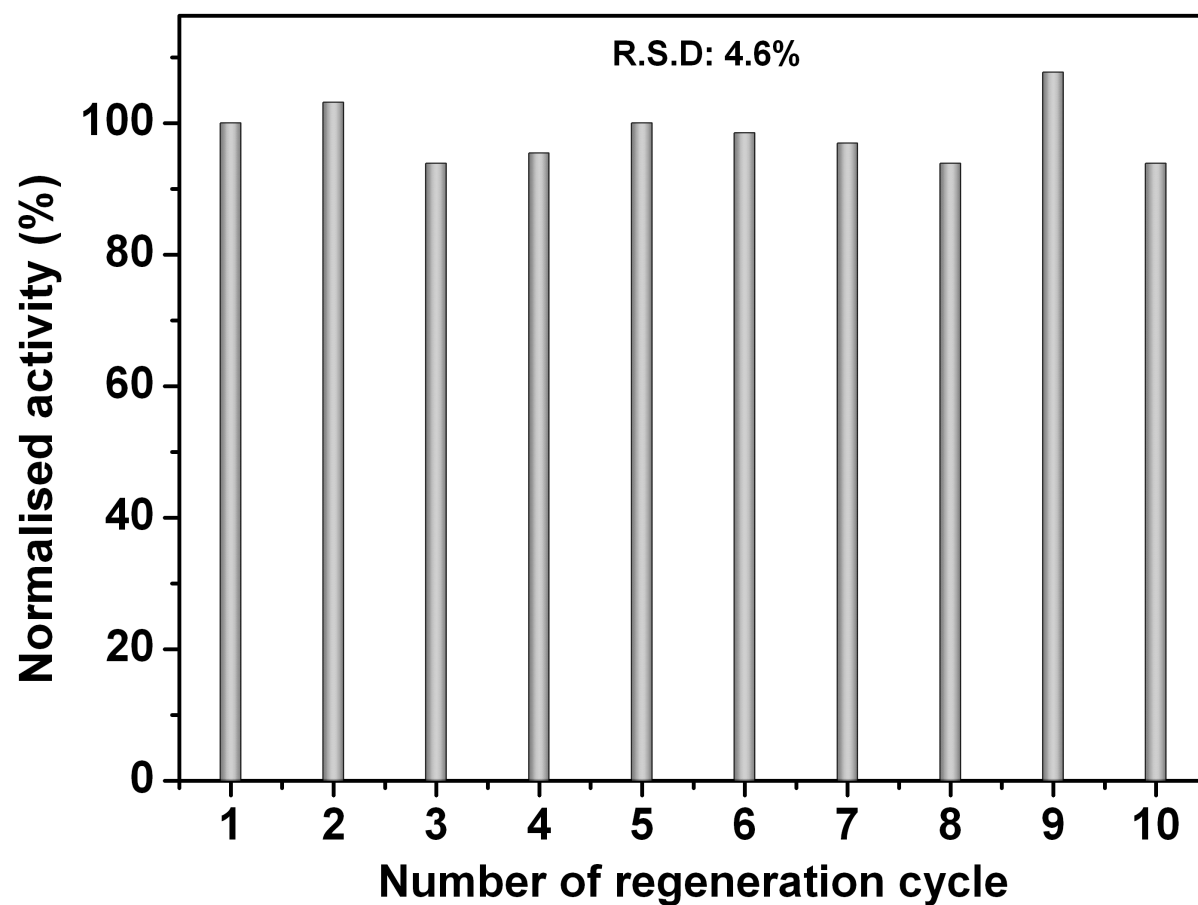


Fig. 6. Regeneration of an NPG/silica/lipase electrode. The response was measured by immersion of the electrode in 2 mL of 75 μ M 4-NPB for 1 h.